Structural and Functional Roles of Deamidation and/or Truncation of N- or C-Termini in Human αA-Crystallin[†]

Jose M. Chaves, Kiran Srivastava, Ratna Gupta, and Om P. Srivastava*

Department of Vision Sciences, University of Alabama at Birmingham, Birmingham, Alabama 35294

Received February 1, 2008; Revised Manuscript Received June 23, 2008

ABSTRACT: The purpose of the study was to compare the effects of deamidation alone, truncation alone, or both truncation and deamidation on structural and functional properties of human lens αA-crystallin. Specifically, the study investigated whether deamidation of one or two sites in αA-crystallin (i.e., αA-N101D, αA-N123D, αA-N101/123D) and/or truncation of the N-terminal domain (residues 1−63) or C-terminal extension (residues 140−173) affected the structural and functional properties relative to wild-type (WT) αA. Human WT-αA and human deamidated αA (αA-N101D, αA-N123D, αA-N101/123D) were used as templates to generate the following eight N-terminal domain (residues 1−63) deleted or C-terminal extension (residues 140−173) deleted αA mutants and deamidated plus N-terminal domain or C-terminal extension deleted mutants: (i) αA-NT (NT, N-terminal domain deleted), (ii) αA-N101D-NT, (iii) αA-N123D-NT, (iv) αA-N101/123D-NT, (v) αA-CT (CT, C-terminal extension deleted), (vi) αA-N101D-CT, (vii) αA-N123D-CT, and (viii) αA-N101/123D-CT. All of the proteins were purified and their structural and functional (chaperone activity) properties determined. The desired deletions in the αA-crystallin mutants were confirmed by matrix-assisted laser desorption/ionization-time-of-flight (MALDI-TOF) mass spectrometric analysis. Relative to WT-αA homomers, the mutant proteins exhibited major structural and functional changes. The maximum decrease in chaperone activity in homomers occurred on deamidation of N123 residue, but it was substantially restored after N- or C-terminal truncations in this mutant protein. Far-UV circular dichroism (CD) spectral analyses generally showed an increase in the *β*-contents in αA mutants with deletions of N-terminal domain or C-terminal extension and also with deamidation plus above N- or C-terminal deletions. Intrinsic tryptophan (Trp) and total fluorescence spectral studies suggested altered microenvironments in the αA mutant proteins. Similarly, the ANS (8-anilino-1-naphthalenesulfate) binding showed generally increased fluorescence with blue shift on deletion of the N-terminal domain in the deamidated mutant proteins, but opposite effects were observed on deletion of the C-terminal extension. Molecular mass, polydispersity of homomers, and the rate of subunit exchange with WT-αB-crystallin increased on deletion of the C-terminal extension in the deamidated αA mutants, but on N-terminal domain deletion these values showed variable results based on the deamidation site. In summary, the data suggested that the deamidation alone showed greater effect on chaperone activity than the deletion of N-terminal domain or C-terminal extension of αA-crystallin. The N123 residue of αA-crystallin plays a crucial role in maintaining its chaperone function. However, both the N-terminal domain and C-terminal extension are also important for the chaperone activity of αA-crystallin because the activity was partially or fully recovered following either deletion in the αA-N123D mutant. The results of subunit exchange rates among αA mutants and WT-αB suggested that such exchange is an important determinant in maintenance of chaperone activity following deamidation and/or deletion of the N-terminal domain or C-terminal extension in αA-crystallin.

Among lens crystallins (α-, *β*-, and *γ*-crystallins), only the α-crystallin belongs to a heat shock protein family [HSPs] (*1*) and has chaperone activity (*2*). Like other HSPs, α-crystallin also contains a highly conserved sequence of 80−100 residues called the α-crystallin domain (residues 64−139 in αA-crystallin and residues 66−144 in αB-crystallin) (*3*). Based on similarities with the structures of other HSPs, it is believed that the N-terminal region of both αA- (residues 1−63) and αB- (residues 1−66) crystallins forms independently folded domain, whereas the C-terminal region (residues 143−173 in αA-crystallin and residues 147−175 in αB-crystallin) is flexible and unstructured (*1*). On the removal of N-terminal residues (partial or 1−56 residues of N-terminus) and the C-terminal extension (partial or 32−34 residues of C-terminus) of αA- and αB-crystallins, the proteins showed improper folding, reduced chaperone activity, and formation of trimers or tetramers (*4–8*). Residues 42−57 and residues 60−71 of αB-crystallin interact with αA-crystallin (*9, 10*), and pin-array analysis has further shown that five peptide sequences of αB-crystallin (i.e., residues 37−54 [in the N-terminal region], residues 75−82, 131−138, 141−148 [form *β*-strand in the conserved α-crys-

[†] This study was supported by National Eye Institute Grant EY06400 and partly by NIH Grants P50AT00477 and P30EY0339.

* To whom correspondence should be addressed. E-mail: Srivasta@uab.edu. Phone: (205) 975-7630. Fax: (205) 934-5725.

10.1021/bi8001902 CCC: $40.75
Published on Web 08/29/2008

tallin domain], and residues 155−166 [in the C-terminal extension]) interact with αA-crystallin (*11*). In spite of these studies, the individual amino acids in the αA and αB subunits that interact with target protein during chaperone activity have not been fully identified.

Age-related conformational changes and unfolding of α-, *β*-, and *γ*-crystallins are believed to lead to their aggregation and cross-linking. Two disease-related point mutations of a highly conserved Arg at equivalent positions in αA- (R116C) and αB- (R120G) crystallins caused structural changes that lead to hereditary cataracts (*12, 13*). Changes that are likely due to posttranslational modifications of crystallins, such as disulfide bonding (*14*), glycation (*15*), oxidation of Trp and His residues (*16, 17*), deamidation (*18*), and transglutaminase-mediated cross-linking (*19*), are also believed to cause cataract. Because deamidation has been identified as the most prevalent among posttranslational modifications in human lenses (*1, 17, 20*), it might play a major role during cataractogeneis.

Deamidation introduces a negative charge (i.e., an amide group is replaced with a carboxylic group) that causes changes in protein tertiary structure and, in turn, affects structural and functional properties. For example, the deamidation at critical sites in *β*B2-crystallin destabilized its dimers and, therefore, might disrupt its function in oligomer formation in the lens (*21*). Similarly, our recent studies showed that both Asn residues (at positions N101 and N123) are required for the structural integrity and chaperone function of homoaggregates of human αA-crystallin, and the deamidation of N101 but not of N123 (both present in the conserved region of αA) had profound effects on its structural and functional properties (*22*). We also showed that the deamidation of N146 but not of N78 in human αB-crystallin had profound effects on its structural and functional properties (*23*).

The deamidation of both glutaminyl and aspariginyl residues in proteins might serve as molecular clocks of biological events such as protein turnover, development, and aging (*24*). Indeed, the turnover rates of cytochrome *c* (*25*), rabbit muscle aldose reductase, histones, and erythrocyte membrane protein 4.1 (*26–28*) were accelerated following deamidation. However, as stated above, the age-related deamidation of crystallins (αA and αB, *β*B1, and *γ*S-crystallins) affected their properties as a major posttranslational modification (*18, 22, 23, 29–31*), and deamidation of specific residues increased in the water-insoluble (WI)[1] proteins compared to water-soluble (WS) proteins in human lenses (*32*). This suggested that deamidation could cause structural instability that might lead to insolubilization of a protein. The cataract-specific deamidation of N-143 in *γ*S-crystallin further supports this possibility (*31*).

Although the deamidation but not the truncation has been shown to cause structural changes leading to insolubilization of *β*B1-crystallin (*33*), similar effects on αA- or αB-crystallins are presently unknown. *In vivo*, both αA- and αB-crystallins show relatively greater susceptibility to degradation of the C-terminal region than of the N-terminal region (*34–36*). However, presently, no clear link exists between the greater susceptibility of C-terminal region of deamidated vs nondeamidated αA- or αB-crystallins to their cleavage via enzymatic/nonenzymatic reactions. Therefore, the question of the relative effects of deamidation and/or truncation on the structural and functional properties of αA and αB-crystallins remains unanswered. Because truncation or mutation in the C-terminal extension of α-sHSPs has resulted in myopathies and cataract (*37, 38*), and the N-terminal extension in various sHSPs plays a major function in multimeric complex formation (*39*), it is important to understand the effects of deletion of N-terminal domain or C-terminal extension of α-crystallin on its chaperone activity. To answer this question, the purpose of the present study was to examine relative effects of deamidation alone, N- or C-terminal deletion, and deamidation plus N- or C-terminal deletion on structural and functional properties of αA-crystallin. Using the αA-deamidated mutants (i.e., αA-N101D, αA-N123D, or αA-N101/123D) (*23*), we generated deamidated plus either N-terminal domain- (residues 1−63) or C-terminal extension- (residues 140−173) deleted mutants. Additionally, the N-terminal domain- or C-terminal extension-deleted mutants of WT-αA crystallin were also generated to be used as controls. This report describes comparative structural and functional properties of the WT-αA crystallin and its mutant proteins.

EXPERIMENTAL PROCEDURES

Materials. The restriction endonucleases *Apa*I, *Sac*I, and *Sph*I, the molecular weight protein markers, and DNA markers were purchased from either Amersham Biosciences (Piscataway, NJ) or Promega (Madison, WI). The T7 promoter, T7 terminator, and other primers used in the study were obtained from Sigma Genosis (St. Louis, MO). All chemicals for gel electrophoresis were from Amersham Biosciences (Piscataway, NJ) or Bio-Rad (South San Francisco, CA). Unless indicated otherwise, all other molecular biology grade chemicals used in this study were purchased from Fisher (Atlanta, GA) or Sigma (St. Louis, MO) companies.

Bacterial Strains and Plasmids. Escherichia coli BL21(DE3) bacterial strain was obtained from Invitrogen (Carlsbad, CA). The human αA-crystallin cDNA cloned on a plasmid pDIRECT was received from Dr. Mark Petrash, Washington University, St. Louis, MO. Cells were propagated in Luria broth, and recombinant bacteria were selected using ampicillin.

Site-Specific Mutagenesis. Deamidation of Asn (N) at positions 101, 123, and at both positions to Asp (D) was introduced in αA-cDNA using a QuikChange site-directed mutagenesis kit (Stratagene, La Jolla, CA) as described previously (*23*). The deamidated αA DNA was used as templates, with specific complementary primer pairs (Table 1) to generate the desired deleted or deamidated plus deleted αA-crystallin mutants. The PCR products were ligated to pET 100 Directional TOPO vector. Recombinant human αA-crystallin coding sequence (WT-αA), αA-N101D, αA-N123D, and αA-N101/123D were subcloned in the pET100 Directional TOPO vector to introduce His tags. Also, the N-terminal domain (residues 1−63) or the C-terminal extension (residues 140−173) was deleted in WT-αA and the

[1] Abbreviations: 8-anilino-1-naphthalenesulfate (ANS), daltons (Da), dithiothreitol (DTT), isopropyl *β*-D-1-thiogalactopyranoside (IPTG), matrix-assisted laser desorption/ionization-time-of-flight (MALDI-TOF), multiangle light scattering (MALS), sodium dodecyl sulfate−polyacrylamide gel electrophoresis (SDS−PAGE), small heat shock proteins (sHSPs), water insoluble (WI), water soluble (WS), wild type (WT).

Table 1: Oligonucleotide Primers[a]

deletion mutant constructs		primers (5′−3′)
WT-αA	forward	CACCATGGACGTGACCATCCAGCACCCCTG
	reverse	TAGGACGAGGGAGCCGAGGTGGGC
αA-N101D	forward	CACCATGGACGTGACCATCCAGCACCCCTG
	reverse	TAGGACGAGGGAGCCGAGGTGGGC
αA-N123D	forward	CACCATGGACGTGACCATCCAGCACCCCTG
	reverse	TAGGACGAGGGAGCCGAGGTGGGC
αA-N101/123D	forward	CACCATGGACGTGACCATCCAGCACCCCTG
	reverse	TAGGACGAGGGAGCCGAGGTGGGC
αA-NT	forward	CACCGTTCGATCCGACCGGGACAAGTTCG
	reverse	TTAGGACGAGGGAGCCGAGGTGGGC
αA-N101D-NT	forward	CACCGTTCGATCCGACCGGGACAAGTTCG
	reverse	TTAGGACGAGGGAGCCGAGGTGGGC
αA-N123D-NT	forward	CACCGTTCGATCCGACCGGGACAAGTTCG
	reverse	TTAGGACGAGGGAGCCGAGGTGGGC
αA-N101/123D-NT	forward	CACCGTTCGATCCGACCGGGACAAGTTCG
	reverse	TTAGGACGAGGGAGCCGAGGTGGGC
αA-CT	forward	CACCATGGACGTGACCATCCAGCACCCCTG
	reverse	TTAGGTCAGCATGCCATCGGCAGACAGGG
αA-N101D-CT	forward	CACCATGGACGTGACCATCCAGCACCCCTG
	reverse	TTAGGTCAGCATGCCATCGGCAGACAGGG
αA-N123D-CT	forward	CACCATGGACGTGACCATCCAGCACCCCTG
	reverse	TTAGGTCAGCATGCCATCGGCAGACAGGG
αA-N101/123D-CT	forward	CACCATGGACGTGACCATCCAGCACCCCTG
	reverse	TTAGGTCAGCATGCCATCGGCAGACAGGG

[a] These primers were used for subcloning WT-αA and deamidated αA-species, and generating the truncated αA mutant proteins using PCR-based mutagenesis. NT denotes the N-terminally truncated and CT denotes the C-terminally truncated mutant proteins.

deamidated mutants to generate N-terminal domain- or C-terminal extension-deleted mutants using PCR-based mutagenesis. Thus, the following eight mutants were generated: (i) αA-NT (NT, N-terminally [residues 1−63] truncated), (ii) αA-N101D-NT, (iii) αA-N123D-NT, (iv) αA-N101/123D-NT, (v) αA-CT (CT, C-terminally [residues 140−173] truncated), (vi) αA-N101D-CT, (vii) αA-N123D-CT, and (viii) αA-N101/123D-CT. Briefly, 25 ng of template was used, and the PCR conditions were as follows: predenaturing at 95 °C for 30 s, followed by 30 cycles of denaturing at 95 °C for 30 s, annealing at 60−64 °C (depending on the melting temperature [T_m] of the primers) for 30 s, and extensions at 72 °C for 1 min followed by a final extension at 72 °C for 10 min. The PCR products were ligated into the pET100 Directional TOPO vector (Invitrogen) using the manufacturer's instructions, and the positive clones were identified by restriction analysis using *Apa*I, *Sac*I, and *Sph*I. The orientation of the DNA sequences was confirmed by their sequencing at the Core Facility of the University of Alabama at Birmingham.

Expression and Purification of Wild-Type and Mutant Proteins. E. coli BL21(DE3) was transformed with mutant amplicons using a standard *E. coli* transformation procedure as described previously (*22, 23*). The proteins were overexpressed by addition of isopropyl β-D-1-thiogalactopyranoside (IPTG, final concentration of 1 mM), and the cultures were incubated further at 37 °C for 4 h. The cells were harvested and resuspended in lysis buffer [50 mM Tris-HCl (pH 8.0) containing lysozyme (0.25 mg/mL) and protease inhibitor cocktail (Sigma)] and lysed by sonication at 5 °C. DNA was degraded using DNase I (10 μg/mL) and incubation on ice for 30 min. The soluble fraction was separated by centrifugation at 8000*g* for 15 min at 5 °C, and the pellet was resuspended in a detergent buffer [0.02 M Tris-HCl, pH 7.5, containing 1% (w/v) sodium deoxycholate, 0.2 M NaCl, and 1% NP-40]. The detergent-soluble fraction was separated by centrifugation at 5000*g* for 10 min at 5 °C; the pellet was washed with 0.5% Triton X-100 (10 μg of DNase I was added if the pellet was viscous). The washing of the pellet was repeated as necessary to remove bacterial debris from the inclusion bodies. The pellet was resuspended in denaturation buffer [DB buffer: 0.02 M sodium phosphate, pH 7.8, containing 8 M urea and 0.5 M NaCl].

Depending on the expression of the desired mutant proteins either in soluble fraction or in the inclusion bodies, they were purified under either native or denaturing conditions. In case the desired protein was expressed as partly soluble form (i.e., present in both soluble fraction and inclusion bodies), the soluble protein fraction was selectively used for its purification. All purification steps, including refolding of proteins, were carried out at 5 °C unless indicated otherwise. Each of the mutant proteins contained six His tags and was purified by an affinity chromatographic method using Pro-bond Ni^{2+} chelating column as described by the manufacturer (Invitrogen). Briefly, during purification under native conditions, a column was equilibrated with native buffer (NB buffer: 20 mM sodium phosphate [pH 7.8] containing 0.5 M NaCl), the protein preparation was applied to the column and then washed with NB containing 10 mM imidazole, and finally, the matrix-bound protein was eluted with NB containing 250 mM imidazole (pH 7.8). During purification of a mutant protein under denaturing conditions, the column was equilibrated with DB buffer. Following protein application, the unbound proteins were eluted, first with DB buffer, which was followed by a second wash with DB buffer at pH 6.0 (pH adjusted with HCl) and a third wash with DB buffer at pH 5.3 (pH adjusted with HCl). The bound proteins were eluted with DB buffer (pH 7.8) containing 250 mM imidazole. SDS−PAGE analysis (*40*) was used to identify the fractions that contained the desired proteins during purification. The proteins purified under native conditions were pooled, dialyzed against 0.05 M phosphate buffer (pH 7.5) at 5 °C, and stored at −20 °C until used. The proteins purified under denaturing conditions were folded as described below.

Refolding of Mutant Proteins Purified under Denaturating Conditions. The purified mutant proteins purified under denaturating conditions were refolded in a urea-free buffer. Briefly, a desired protein was refolded by adding it dropwise to an excess of cold buffer (25 mM Tris-HCl, 1 mM DTT, pH 7.5) at 1:100 dilution (denatured protein:buffer). Circular dichroism spectrum was recorded to determine whether a refolded WT-αA had a similar secondary structure to that of its native form.

Determination of Structural and Functional Properties of WT-αA-Crystallin and Mutant Proteins. (1) Fluorescence Studies. All fluorescence spectra were recorded in corrected spectrum mode using a Shimadzu RF-5301PC spectrofluorometer with excitation and emission band passes set at 5 and 3 nm, respectively. The intrinsic Trp fluorescence intensities of the WT-αA, the three deamidated mutants, and the deamidated plus C-terminal extension-deleted αA mutants (0.15 mg/mL of each), each dissolved in 10 mM sodium phosphate buffer, pH 7.4, containing 100 mM NaCl, were recorded with an excitation at 295 nm and emission between 300 and 400 nm. Because human αA-crystallin contains a single Trp at position 9 that was lost during deletion of the N-terminal domain (residues 1−63), the total fluorescence intensities of the N-terminally deleted mutants and their controls were recorded with an excitation at 285 nm and emission between 300 and 400 nm.

(2) ANS-Binding Studies. The binding of a hydrophobic probe, ANS, to WT-αA and mutant proteins was determined by recording fluorescence spectra after excitation at 390 nm and emission between 400 and 600 nm. In these experiments, 15 μL of 0.8 mM ANS (dissolved in methanol) was added to a protein preparation (0.15 mg/mL, dissolved in 10 mM phosphate buffer, pH 7.4). The samples were incubated at 37 °C for 15 min prior to the fluorescence measurements.

(3) Circular Dichroism (CD) Studies. To investigate the secondary structural changes in the WT-αA and mutant proteins, their far-UV CD spectra were determined at room temperature using a AVIS spectropolarimeter (Model 62DS, Lakewood, NJ). The αA-crystallin preparations at 0.2−0.3 mg/mL (dissolved in 50 mM Tris-HCl, pH 7.9) were used for recording the far-UV CD spectra. The path length was 0.1 cm during the far-UV CD spectra determination. The spectra reported are the average of five scans, corrected for buffer blank and smoothed. Secondary structures were estimated using the SELCON program (*41*).

(4) Oligomer Size Determination by Static Light Scattering. A multiangle laser light scattering instrument (Wyatt Technology, Santa Barbara, CA), coupled to HPLC, was used to determine the absolute molar mass of WT-αA and its mutant proteins. Briefly, protein samples in 50 mM sodium phosphate, pH 7.4, were filtered thorough a 0.22 μm filter prior to their analysis. Results used 18 different angles, and the angles were normalized with the 90° detector.

(5) Chaperone Activity Assay. The chaperone activity was determined by using insulin as the target protein essentially by the methods previously described (*22, 23*). The aggregation of insulin by 20 mM DTT at 25 °C in either the absence or presence of different αA-crystallin species homoaggregates (i.e., WT-αA, αA-N101D, αA-N123D, αA-N101/123D, αA-NT, αA-N101D-NT, αA-N123D-NT, αA-N101/123D-NT, αA-CT, αA-N101D-CT, αA-N123D-CT, and αA-N101/123D-CT mutants) at varying concentrations was determined. The aggregation was monitored as turbidity at 360 nm up to 180 min using a Shimadzu UV−vis scanning spectrophotometer (model UV2101 PC), equipped with a six-cell positioner (Shimadzu model CPS-260) and a temperature controller (Shimadzu model CPS 260). The chaperone activity of heteromers (αA- and αB-crystallins at 3:1 ratio) was also determined as previously described (*22*). For this experiment, the purified WT-αA or the mutant proteins were mixed with purified WT-αB in a 3:1 ratio (αA:αB), followed by denaturation in 4 M guanidine hydrochloride (GdnHCl) and renaturation as described by Bera et al. (*42*). Using this method, the heteromer formation between the following species at a ratio of 3:1 (αA:αB) was examined: (a) WT-αA:WT-αB; (b) αA-N101D:WT-αB; (c) αA-N123D:WT-αB; (d) αA-N101/123D:WT-αB; (e) αA-NT:WT-αB; (f) αA-CT:WT-αB; (g) αA-N101D-NT:WT-αB; (h) αA-N101D-CT:WT-αB; (i) αA-N123D-NT:WT-αB; (j) αA-N123D-CT:WT-αB; (k) αA-N101/123D-NT:WT-αB, and (l) αA-N101/123D-CT:WT-αB. Briefly, the individual heteromer preparations were mixed to 4 M GdnHCl (final concentration) and incubated at room temperature for 6 h. This was followed by dialysis against 50 mM phosphate buffer, pH 7.5, at 5 °C for 24 h with four changes of the buffer.

(6) Subunit Exchange Rates between Recombinant WT-αA, Its Mutants, and WT-αB-Crystallin. The rates of subunit exchange between αA-crystallin (WT and its mutants) and WT-αB were measured using the fluorescence resonance energy transfer (FRET) technique as described previously (*9, 43*). WT-αA and its mutants were labeled with Alexa fluor 350 and acted as energy donors, whereas αB labeled with Alexa fluor 488 acted as an energy acceptor. The fluorescent αA-350 (wild type/mutants) and αB-488 mixture was prepared in 3:1 ratio to mimic the *in vivo* situation, and subunit exchange was monitored at 37 °C in buffer A (50 mM sodium phosphate, pH 7.5, containing 100 mM sodium chloride and 2 mM DTT) for 2 h. The time-dependent decrease in donor fluorescence and concomitant increase in the acceptor fluorescence were monitored upon exciting the samples at the donor absorption maximum (346 nm). After curve fitting of the raw data and nonlinear regression analysis (using Sigma plot 8.0 software), we then calculated the subunit exchange rate.

Purified WT-αA and its mutants were labeled with Alexa fluor 350, and WT-αB was labeled with Alexa fluor 488 using a manufacturer-recommended procedure (Molecular Probes). Briefly, a desired protein was mixed with Alexa fluor dye in 50 mM sodium phosphate with 100 mM sodium bicarbonate. The reaction was allowed to proceed in dark for 2 h at room temperature, and it was stopped by adding 1.5 M hydroxylamine, pH 8.5, and incubation for 1 h at room temperature. The excess of Alexa fluor dye was separated from the labeled proteins by dialyzing against 50 mM phosphate buffer at 5 °C for 48 h with two changes of the buffer using Spectra/Por membrane (3500 Da molecular mass cutoff).

RESULTS

Confirmation of Specific Deletions at Desired Sites in αA-Crystallin Mutants. The three deamidated αA mutants (i.e., αA-N101D, αA-N123D, and αA-N101/123D), generated previously in our laboratory (*22*), were used as templates to

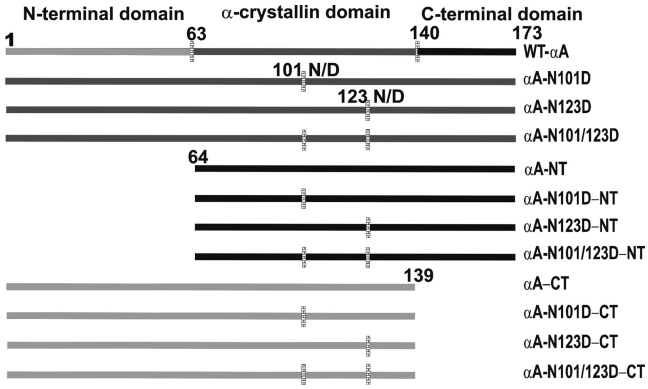

FIGURE 1: Schematic diagram to show the regions and residue numbers forming the N-terminal domain and C-terminal extension and deamidation sites in the WT and 11 mutant proteins (identified by their names on the right). In the three deamidated mutants, N101 or N123 or both were deamidated to D residue. Among the four N-terminal domain-deleted mutants (missing residues 1−63), the first was with no deamidation, and the second, third, and fourth were with the deletion and deamidation at N101, N123, or both to D, respectively. Among the four C-terminal extension-deleted mutants (missing residues 140−173), the first was with no deamidation, and the second, third, and fourth were with the deletion and deamidation at N101, N123, or both to D, respectively.

generate eight either N-terminal domain-deleted or C-terminal extension-deleted mutants (see Experimental Procedures). As shown in Figure 1, the single N-terminal (NT) domain-deleted and the three deamidated plus N-terminal domain-deleted mutants are referred to throughout the text as αA-NT, αA-N101D-NT, αA-N123D-NT, and αA-N101/123D-NT mutants, respectively. Similarly, the single C-terminal (CT) extension-deleted and the three deamidated plus C-terminal extension-deleted mutants are referred to as αA-CT, αA-N101D-CT, αA-N123D-CT, and αA-N101/123D-CT mutants, respectively.

The DNA sequencing results confirmed desired deletions of either N-terminal domain or C-terminal extension in the WT-αA crystallin and in the three deamidated mutants. To confirm the deletions in the expressed mutant proteins, individual protein bands with desired molecular weights, which showed higher expression on IPTG-treatment compared to untreated preparations on a SDS gel, were analyzed by MALDI-TOF mass spectrometry. Figure 2 shows MALDI-TOF mass spectrometric profiles of tryptic fragments of the following three representative proteins: (A) WT-αA, (B) αA-NT mutant protein, and (C) αA-CT mutant protein. The tryptic fragments of WT-αA with mass (Da) of 980.6 (residues 71−78), 1037.5 (residues 13−21), 1090.5 (residues 104−112), 1193.6 (residues 12−21), 1311.7 (residues 146−157), and 1627.7 (residues 100−112) are shown in Figure 2A, which confirmed the full length of WT-αA crystallin. Similarly, the αA-NT mutant protein showed (Figure 2B) tryptic fragments with mass of 981.2 (residues 71−78), 1091.1 (residues 104−112), 1312.4 (residues 146−157), and 1626.7 (residues 100−112). The mutant protein showed an absence of the N-terminal tryptic fragment with mass of 1037.5 (residues 13−21) and 1193.6 (residues 12−21), which suggested the deletion of the N-terminal domain. Similar MALDI-TOF analysis of αA-CT mutant protein (Figure 2C) showed tryptic fragments with mass of 980.7 (residues 71−78), 1037.6 (residues 13−21), 1091.6 (residues 104−112), 1193.7 (residues 12–21), and 1627.8

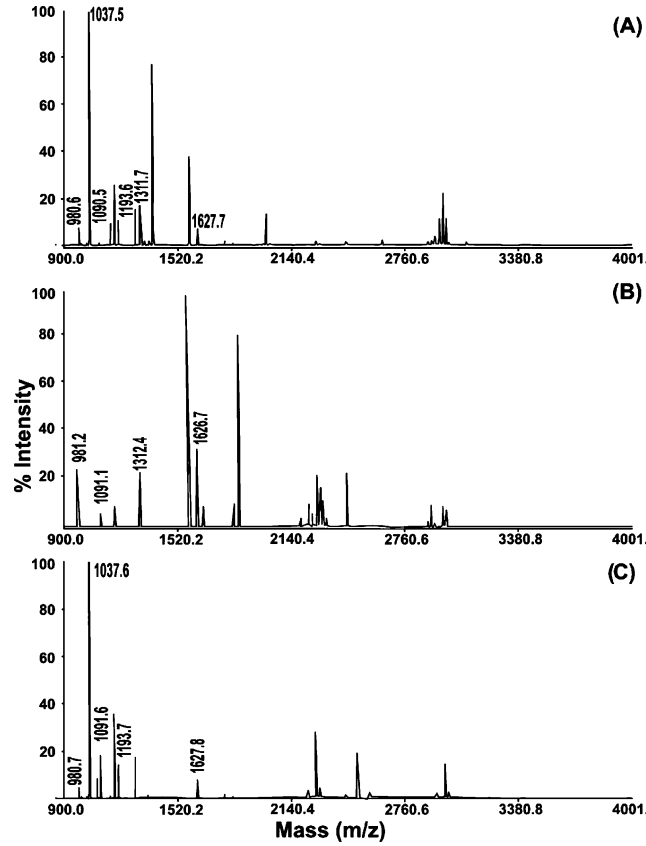

FIGURE 2: Deletions in individual mutant proteins were confirmed by MALDI-TOF mass spectrometry. (A) Typical profile of WT-αA containing the tryptic fragments with masses (Da) 980.6 (residues 71−78), 1037.5 (residues 13−21), 1090.5 (residues 104−112), 1193.6 (residues 12−21), 1311.7 (residues 146−157), and 1626.7 (residues 100−112). (B) Typical profile of αA-NT mutant containing the tryptic fragments with masses 981.2 (residues 71−78), 1091.1 (residues 104−112), 1312.4 (residues 146−157), and 1627.7 (residues 100−112), while missing 1037.5 (residues 13−21) and 1193.6 (residues 12−21). (C) Typical profile of αA-CT mutant containing the tryptic fragments with masses 980.7 (residues 71−78), 1037.6 (residues 13−21), 1091.6 (residues 104−112), 1193.7 (residues 12–21), and 1627.8 (residues 100−112), while missing 1311.7 (residues 146−157).

(residues 100−112). An absence of the C-terminal fragment with mass of 1311.7 (residues 146−157) in the mutant suggested the deletion of C-terminal extension. Similar MALDI-TOF analyses confirmed specific deletions in the remaining six αA mutant proteins (results not shown).

Expression and Purification of Human WT-αA and Mutant Proteins. On expression of WT-αA crystallin and the mutant proteins in *E. coli*, the mutant proteins were recovered in either the soluble or insoluble (inclusion bodies) fractions or in both (Table 2). The deamidated plus N-terminal domain-deleted mutants (αA-NT, αA-N101D-NT, and αA-N123D-NT) were recovered in the soluble fraction, but the deamidated plus C-terminal extension-deleted mutants (αA-CT, αA-N101D-CT, αA-N123D-CT, and αA-N101/123D-CT mutants) were present in the inclusion bodies, suggesting a soluble nature of the former proteins but insoluble nature of the latter proteins. However, the αA-N123D and αA-N101/123D-NT mutant proteins were present in both the soluble fraction and inclusion bodies, suggesting their partial soluble nature. Each protein was purified using a Ni^{2+}-affinity column under native or denaturing conditions as described in Experimental Procedures. In some cases, two consecutive

Table 2: Solubility of WT-αA and Its Deamidated/Deamidated plus N-Terminal Domain- or C-Terminal Extension-Deleted Mutant Proteins[a]

WT-αA and deamidated/ deamidated-deleted mutants	soluble fraction	inclusion bodies
WT-αA	+	−
αA-N101D	−	+
αA-N123D	+	+
αA-N101/123D	−	+
αA-NT	+	−
αA-N101D-NT	+	−
αA-N123D-NT	+	−
αA-N101/123D-NT	+	+
αA-CT	−	+
αA-N101D-CT	−	+
αA-N123D-CT	−	+
αA-N101/123D-CT	−	+

[a] The + sign indicates the presence of the protein as observed on SDS−PAGE after centrifugation.

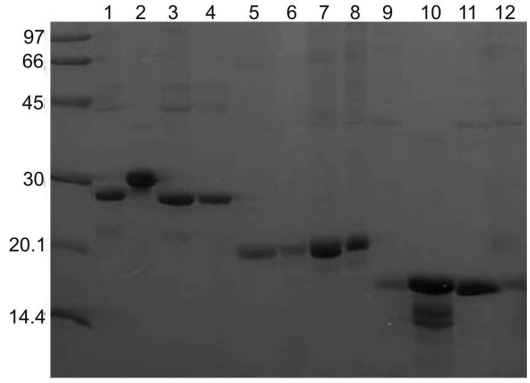

FIGURE 3: SDS−PAGE analysis of WT-αA, its deamidated mutants, and their N- and C-terminally deleted mutant proteins. Lane 1, WT-αA; lane 2, αA-N101D; lane 3, αA-N123D; lane 4, αA-N101/123D; lane 5, αA-CT; lane 6, αA-N101D-CT; lane 7, αA-N123D-CT; lane 8, αA-N101/123D-CT; lane 9, αA-NT; lane 10, αA-N101D-NT; lane 11, αA-N123D-NT; lane 12, αA-N101/123D-NT.

Ni^{2+}-affinity chromatographic steps were needed to recover a desired purified protein species.

The purified WTαA-crystallin and its three deamidated mutant proteins (containing residues 1−173) showed molecular masses of 25−30 kDa on SDS−PAGE analysis (Figure 3, lanes 1 to 4), whereas species with either deletion of the N-terminal domain (residues 1−63) or the C-terminal extension (residues 140−173) showed lower molecular masses of 17−20 kDa (Figure 3, lanes 5−12). As evident from SDS−PAGE analysis (Figure 3), the WT-αA and its mutant proteins were recovered in the highly purified forms, and their higher than expected molecular masses were due to additional six His residues.

Effects of Deletion of N-Terminal Domain or C-Terminal Extension in Deamidated αA-Crystallin Mutants on Their Structural and Functional Properties. (1) Comparison of Effects on Chaperone Activity of Deamidation or Deamidation plus Deletions of N-Terminal Domain or C-Terminal Extension. The chaperone activities of WT-αA and its mutant proteins were compared using insulin as a target protein at four different ratios of crystallin to insulin (i.e., 0.25:1, 0.5:1, 0.75:1, and 1:1 [w/w]). The aggregation of insulin alone by DTT was taken as the 0% protection, and relative to this, the percent protection by each of the homoaggregates (WT-αA or its mutant proteins) or heteroaggregates (WT-αA or its mutant proteins plus WT-αB) was calculated. Although only the percent protection of denaturation of insulin by DTT in the presence of αA-crystallin species at 200 μg at the crystallin-to-insulin ratios of 1:1 (w/w) are shown, at other ratios of 0.25:1, 0.5:1, and 0.75:1, similar trends in percent protection were observed. The homomers of WT-αA crystallin exhibited about 90% protection of the DTT-induced denaturation of insulin, which was referred to as the control level, and the protections by other proteins relative to the control were determined. The relative loss of chaperone activity on deamidation of αA-crystallin was similar to those we reported previously (*22*). While the αA-N123D mutant showed complete loss of the chaperone activity (i.e., showed no protection), only 30% protection by αA-N101D and about 70% by αA-N101/123D relative to the control were observed. On the deletion of N-terminal domain, the αA-NT protein exhibited only about 35% protection, but on deletion of C-terminal extension, the αA-CT showed 100% protection (i.e., at the level of the control [WT-αA crystallin]). Together, the results suggested that a maximum loss in chaperone activity of αA-crystallin occurred following deamidation of N123, followed by deletion of the N-terminal domain (residues 1−63), but none occurred on the deletion of C-terminal extension (residues 140−173) (Table 3).

When the N-terminal domain was deleted in the deamidated αA species, they generally exhibited a lower chaperone activity relative to WT-αA control. However, these mutants showed decreasing levels of activity in the following order: αA-N101/123D-NT > αA-N123D-NT > αA-N101D-NT (i.e., percent protection: 89% αA-N101/123D-NT, 87% αA-N123D-NT, and 60% αA-N101D-NT, Table 3). These results also showed that the deamidated plus N-terminal domain-deleted αA species showed higher activity than αA species with only N-terminal deletion, suggesting a gain in the chaperone activity. In contrast to the N-terminal domain deletion, the C-terminal extension deletion in αA-crystallin showed the same level of activity as the WT-αA-crystallin. Surprisingly, the αA-N123D mutant, which lost all of its activity on deamidation, regained its activity on C-terminal deletion to the level of WT-αA-crystallin. In summary, the deamidated plus C-terminal deleted mutants showed decreasing levels of activity in the following order: αA-N101D-CT > αA-N101/123D-CT > αA-N123D-CT (i.e., percent protection: 76% αA-N101D-CT, 54% αA-N101/123D-CT, and 42% αA-N123D-NT, Table 3).

As stated above, the deamidation of N123 to D residue alone in αA-crystallin resulted in a complete loss in chaperone activity relative to WT-αA but on the deletion of N-terminal domain showed relatively lesser loss in activity while after deletion of C-terminal extension showed a complete regain in activity to the same levels as of WT-αA-crystallin. The results suggested a critical role of the N123 residue and N-terminal domain, compared to C-terminal extension, in maintaining chaperone function of the crystallin. Similarly, the αA-N101D and αA-N101/123D mutant proteins that showed loss of 70% and 30% activities, respectively, regained activities to the control (WT-αA) level on deletion of either the N-terminal domain or C-terminal extension. Together, the results suggested greater effects on chaperone activity from deamidation than from N- or C-terminal deletions.

Table 3: Summary of Structural and Functional Properties of WT-αA and Its Deamidated, Deamidated plus N-Terminal Domain-Deleted, and Deamidated plus C-Terminal Extension-Deleted Mutants

	fluorescence[a] (nm)		ANS binding		chaperone activity (%)		CD spectra						
	Trp	broad spectrum	λ_{max} (nm)	intensity (%)	homomers[b]	heteromers[c]	α-helix	β-sheet	β-turn	random coil	molecular mass[d](Da)	polydispersity	rate of subunit exchange (per min)
WT-αA	345	345	502	100	81.92 ± 6.90	31.11	21	45	15	19	7.0×10^5	1.05	0.0412
αA-N101D	345	347	511	23	30.81 ± 0.68	26.83	5	73	4	18	8.0×10^7	1.27	0.0479
αA-N123D	345	343	490	120	0.42 ± 0.33	28.97	33	40	9	18	6.0×10^5	1.04	0.0188
αA-N101/123D	346	347	490	429	68.88 ± 2.54	13.60	31	43	11	15	1.5×10^8	1.01	0.0754
αA-NT	NA[e]	342	491	404	33.58 ± 3.64	33.79	23	65	3	9	2.7×10^5	1.07	0.0703
αA-N101D-NT	NA[e]	332	509	117	60.01 ± 1.98	93.58	15	53	15	17	3.4×10^5	1.17	0.0878
αA-N123D-NT	NA[e]	333	509	87	84.10 ± 7.95	90.97	16	52	14	18	7.9×10^4	1.03	0.0226
αA-N101/123D-NT	NA[e]	342	497	400	86.67 ± 4.70	78.09	21	47	14	18	2.1×10^7	1.13	0.0258
αA-CT	348	346	524	36	99.9 ± 2.99	59.16	10	64	8	18	1.2×10^8	1.18	0.0742
αA-N101D-CT	342	348	506	76	46.70 ± 2.07	13.24	22	48	13	17	4.0×10^7	1.07	0.0814
αA-N123D-CT	347	344	517	42	98.73 ± 2.49	10.55	44	32	10	14	1.5×10^8	1.41	0.0457
αA-N101/123D-CT	346	347	525	54	85.72 ± 4.01	14.65	6	48	12	34	9.0×10^6	1.17	0.0345

[a] Trp fluorescence was determined for those αA species that contained Trp-9. Broad spectrum was determined in αA species that lacked Trp-9 due to N-terminal domain deletion. [b] Homomers contained only the αA species. [c] Heteromers contained WT-αA or its mutants and WT-αB. [d] Molecular mass was determined by static light scattering method. [e] NA: not applicable.

The chaperone activities of heteromers composed of WT-αA or its mutants plus WT-αB (at 3:1 ratio) were also determined (Table 3). The heteromers were generated as described in Experimental Procedures, and the level of percent protection by heteromers containing WT-αA and WT-αB (referred as the control level) was used to determine relative protection by other heteromers. The level of protection by heteromers of either αA-N101D or αA-N123D plus WT-αB was identical to the control level, whereas it was relatively reduced to half (50%) by the heteromers of αA-N101/123D plus WT-αB-crystallin. This reduced chaperone activity was remarkable because the αA-N101/123D homomers showed only about 30% reduction in activity relative to WT-αA homomers. The results suggested that relative to the control (i.e., heteromers of WT-αA and WT-αB), only the αA-N101/123D mutant showed loss of the activity on heteromer formation with WT-αB-crystallin. As stated above, the homomers of αA-N101D and αA-N123D mutants exhibited 30% and 0% activity relative to homomers of WT-αA, respectively. This suggested that, unlike the αA-N101/123D mutant, the αA-N101D or αA-N123D mutants restored the activity to the control level on oligomerization with WT-αB. Additionally, the activity of heteromers of N-terminal domain-deleted αA-crystallin plus WT-αB-crystallin was at the control levels, but the activity of heteromers of the C-terminal extension-deleted αA and WT-αB was about two times higher than the control level (Table 3). This was in contrast to the activity of homomers of αA-NT and αA-CT, which showed 60% reduction and no reduction in activity, respectively. The activities of heteromers of αA-N101D-NT or αA-N123D-NT plus WT-αB were three times higher than the control levels, which was in contrast to their same levels of activity as the control during homomer formation. This suggested that αA-N101D-NT or αA-N123D-NT became better chaperones than the control on oligomerization with WT-αB. The most intriguing result was that the heteromers of αA-N101D-CT, αA-N123D-CT, or αA-N101/123D-CT plus WT-αB-crystallin showed 50% reduced chaperone activity compared to control levels. Additionally, the chaperone activities of these heteromers were substantially reduced compared with their respective homomers of WT-αA, αA-N101D-CT, αA-N123D-CT, or αA-N101/123D-CT. In summary, the results suggested that oligomerization of the deamidated αA mutants (αA-N101D and αA-N123D but not αA-N101/123D) with αB-crystallin restored the lost activity. Additionally, while the N-terminal domain-deleted deamidated αA became a better chaperone on oligomerization with WT-αB, the C-terminal extension-deleted deamidated αA lost their activity on oligomerization with WT-αB relative to control levels.

(2) Circular Dichroism Spectral Studies. To evaluate the effects of deletion of the N-terminal domain or C-terminal extension on secondary structural changes in WT-αA and its deamidated mutant proteins, the far-UV CD spectra were determined (Figure 4, Table 4). As shown in Table 4 and Figure 4A, the WT-αA-crystallin exhibited 21% α-helix, 45% β-sheet, 15% β-turn, and 19% of random coil contents. In contrast, the αA-N101D mutant showed 5% α-helix, 73% β-sheet, 4% β-turn, and 18% random coil contents, suggesting that the deamidation of N101 augmented the β-sheet content (Figure 4B). The other two deamidated mutant proteins (i.e., αA-N123D and αA-N101/123D) showed

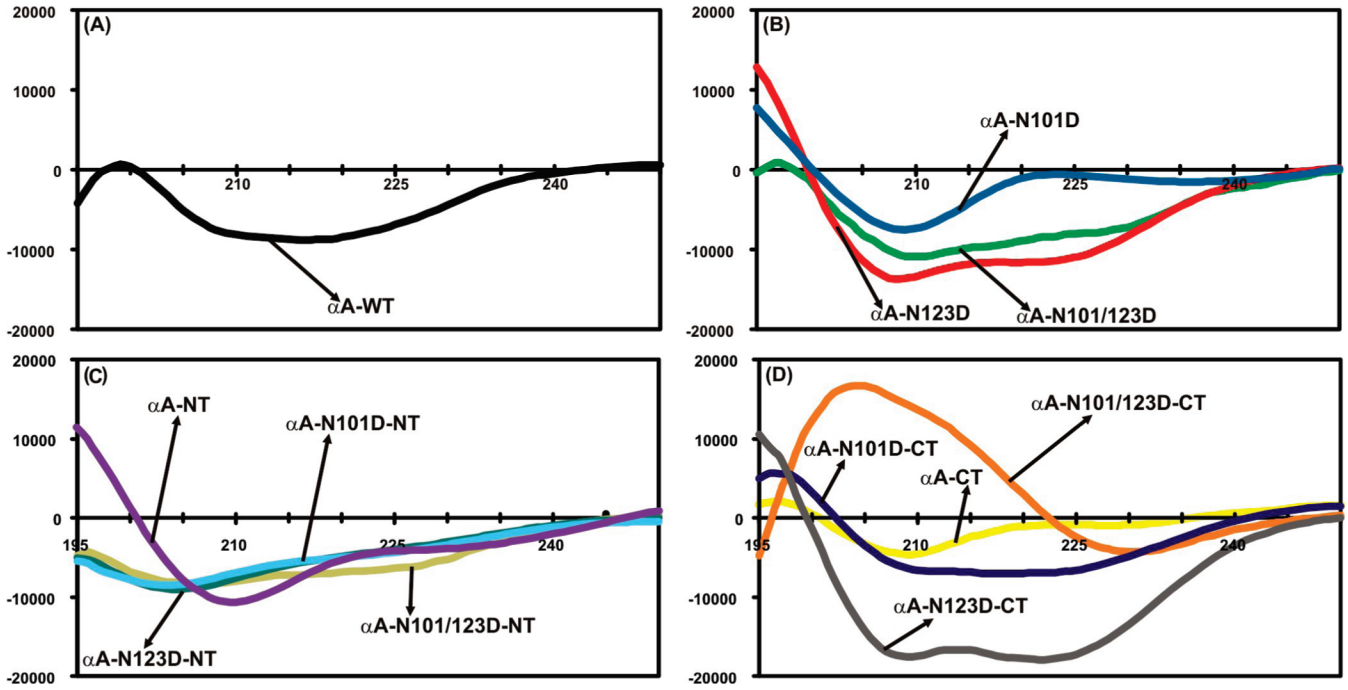

FIGURE 4: Far-UV CD spectra of WT-αA and mutant proteins. The αA-crystallin preparations at 0.2−0.3 mg/mL (dissolved in 50 mM Tris-HCl, pH 7.9) were used for recording the far-UV CD spectra with a path length of 0.1 cm. The spectra reported are the average of five scans, corrected for buffer blank and smoothed.

Table 4: Secondary Structural Contents of WT-αA and Its Mutant Proteins[a]

	α-helix (%)	β-sheet (%)	β-turn (%)	random coil (%)
WT-αA	21	45	15	19
αA-N101D	5	73	4	18
αA-N123D	33	40	9	18
αA-N101/123D	31	43	11	15
αA-NT	23	65	3	9
αA-N101D-NT	15	53	15	17
αA-N123D-NT	16	52	14	18
αA-N101/123D-NT	21	47	14	18
αA-CT	10	64	8	18
αA-N101D-CT	22	48	13	17
αA-N123D-CT	44	32	10	14
αA-N101/123D-CT*	6	48	12	34

[a] These percentages were determined from the far-UV CD spectra of WT-αA and its mutant proteins (0.2−0.3 mg/mL). The asterisk (*) indicates that selcon3 was used instead of selcon.

almost identical β-sheet contents as the WT, but their α-helix contents were increased (i.e., 31% and 33% in the two mutants compared to 21% in WT, Figure 4A,B, Table 4). The deletion of either the N-terminal domain or C-terminal extension resulted in a substantial increase to about 65% in β-sheet contents relative to the 45% of the WT protein, but the α-helix contents in WT-αA and αA-NT were the same (21% and 23%), but it was reduced to 10% in the αA-CT mutant protein (Figure 4C,D). On deletion of the N-terminal domain in the deamidated αA-crystallin species, the β-sheet content increased 47% to 53% in the αA-N101D-NT, αA-N123D-NT, and αA-N101/123D-NT proteins relative to 45% of WT-αA. On deletion of the C-terminal extension in the deamidated αA species, the β-sheet contents increased to 48% in both the αA-N101D-CT and αA-N101/123D-CT proteins, respectively, but it decreased to 32% in αA-N123D-CT protein. However, relative to the WT protein, the α-crystallin contents increased to 44% in αAN123D-CT, remained the same in αA-N101D-CT, and were substantially reduced in αA-N101/123D-CT. Together, the results suggested that N-terminal deletion in WT-αA and in its three deamidated mutant proteins led to greater secondary structural changes than did deletion of C-terminal extension in these proteins.

(3) Determination of Intrinsic Trp Fluorescence Spectra and Broad Spectra. Because αA-crystallin contains a single Trp residue at position 9 in the N-terminal domain (residues 1−63), it was absent in the N-terminal domain-deleted mutants. Therefore, the comparative Trp fluorescence spectra of those species that contained Trp-9 (i.e., WT-αA, αA-N101D, αA-N123D, αA-N101/123D, αA-CT, αA-N101D-CT, αA-N123D-CT, and αA-N101/123D-CT) were determined, and the total spectra (between 300 and 400 nm) of species with no Trp-9 (i.e., αA-NT, αA-N101D-NT, αA-N123D-NT, and αA-N101/123D-NT) were recorded (Figure 5, Table 3). The aromatic rings of amino acids are the primary reasons for the absorbance peak of proteins at 280 nm. Tyr and especially Trp absorb at 280 nm whereas Phe absorbs at 260 nm but not at 280 nm. Further, the λ_{max} fluorescence of Trp is at 340 nm and that of Tyr at 208 nm. However, the λ_{max} for fluorescence of WT-α was at 345 nm and that αA-N123D-NT was at 325 nm. This could be due to exposed Tyr residues in the mutant or alternatively due to certain impurity in the preparations.

On excitation at 295 nm, WT-αA, αA-N101D, αA-N123D, and αA-N101/123D showed identical emission fluorescence with λ_{max} at 345−346 nm (Figure 5A). On deletion of C-terminal extension, αA-N101D-CT, αA-N123D-CT, and αA-N101/123D showed a shift of 3 nm red, 2 nm red, and none in λ_{max}, respectively, suggesting that the deletion resulted in an altered microenvironment around Trp-9 in αA-N101D and αA-N123D but not in αA-N101/123D (Figure 5A, Table 3). The λ_{max} in the total spectra of the Trp-deficient and deamidated-N-terminal deleted species (i.e., αA-NT, αA-N101D-NT, αA-N123D-NT, and αA-

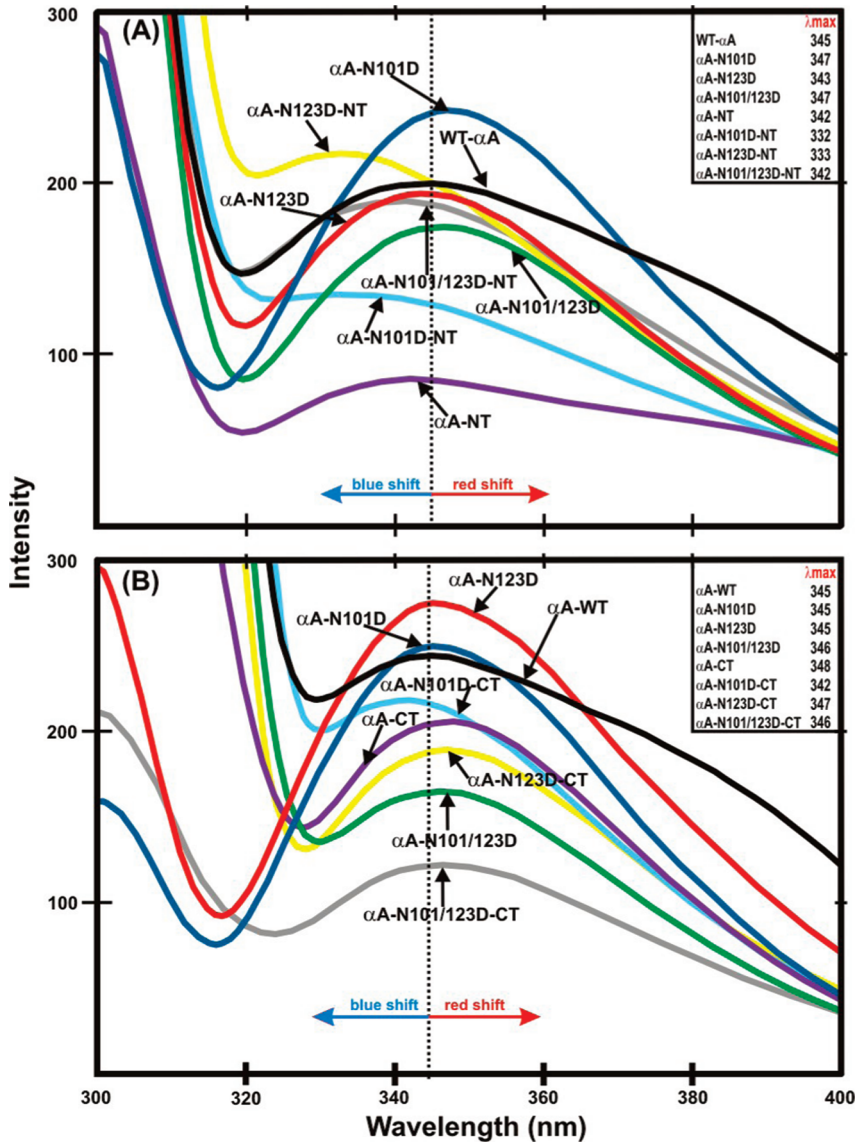

FIGURE 5: Fluorescence studies of WT-αA and mutant proteins. (A) Total fluorescence intensities (Ex 285, Em 300−400) were measured for the N-terminally truncated mutants and their controls because of the deletion of the only Trp at position 9 in the N-terminally truncated mutants. (B) Intrinsic Trp fluorescence intensities (Ex 295, Em 300−400) of C-terminally truncated mutants and their controls. The dotted line indicates the maximum wavelength peak observed in WT-αA.

N101/123D-NT) exhibited blue shift of 3 nm, 13 nm, 12 nm, and 3 nm, respectively (Figure 5B, Table 3). Together, the results suggested that relative to the WT protein, the structures of these mutant proteins were altered more following the deletion of N- or C-terminal regions than following deamidation of either N101 or N123 residues.

(4) Surface Hydrophobicity of WT-αA-Crystallin and Its Mutant Proteins. Because past studies have suggested that interactions between a chaperone molecule (α-crystallin) and a target protein largely involve hydrophobic residues (*10*), the surface hydrophobic patches in WT-αA-crystallin and its mutant proteins were probed by using their binding to ANS (Figure 6, Table 3). Because ANS is nonfluorescent in an aqueous solution but becomes fluorescent when bound to surfaces hydrophobic patches of a protein, it is a useful probe to determine changes in surface hydrophobic patches. On binding to ANS, WT-αA-crystallin showed a fluorescence intensity peak at 502 nm, but the αA-N101D mutant showed a 9 nm red shift to 511 nm with quenching, and both αA-N123D and αA-N101/123D mutants showed a 12 nm blue shift to 490 nm. The results suggested that compared to WT-αA-crystallin, the deamidation of N101 residue resulted in greater exposed surface hydrophobic patches, but the deamidation of only residue N123 or both N101 and N123 residues reduced the surface-exposed hydrophobic patches. Deletion of the N-terminal domain in WT-αA resulted in an 11 nm blue shift with increased fluorescence intensity, but the deletion of C-terminal extension caused a 22 nm red shift with quenching (Table 3). This suggested that, relative to WT-αA, the N-terminal domain-deleted αA mutants had increased surface hydrophobic patches and were relatively reduced in the C-terminal extension-deleted αA. Further, the αA-N101D-NT and αA-N123D-NT mutants showed λ_{max} of 509 nm (a 7 nm red shift), but αA-N101/123D-NT showed λ_{max} of 497 (a 5 nm blue shift), suggesting that the former mutants showed greater hydrophobic patches than the latter on deletion of the N-terminal domain.

Compared to λ_{max} of 502 nm in WT-αA, the deletion of either the N-terminal domain or C-terminal extension resulted in relatively relaxed structures, as represented by a 7 nm

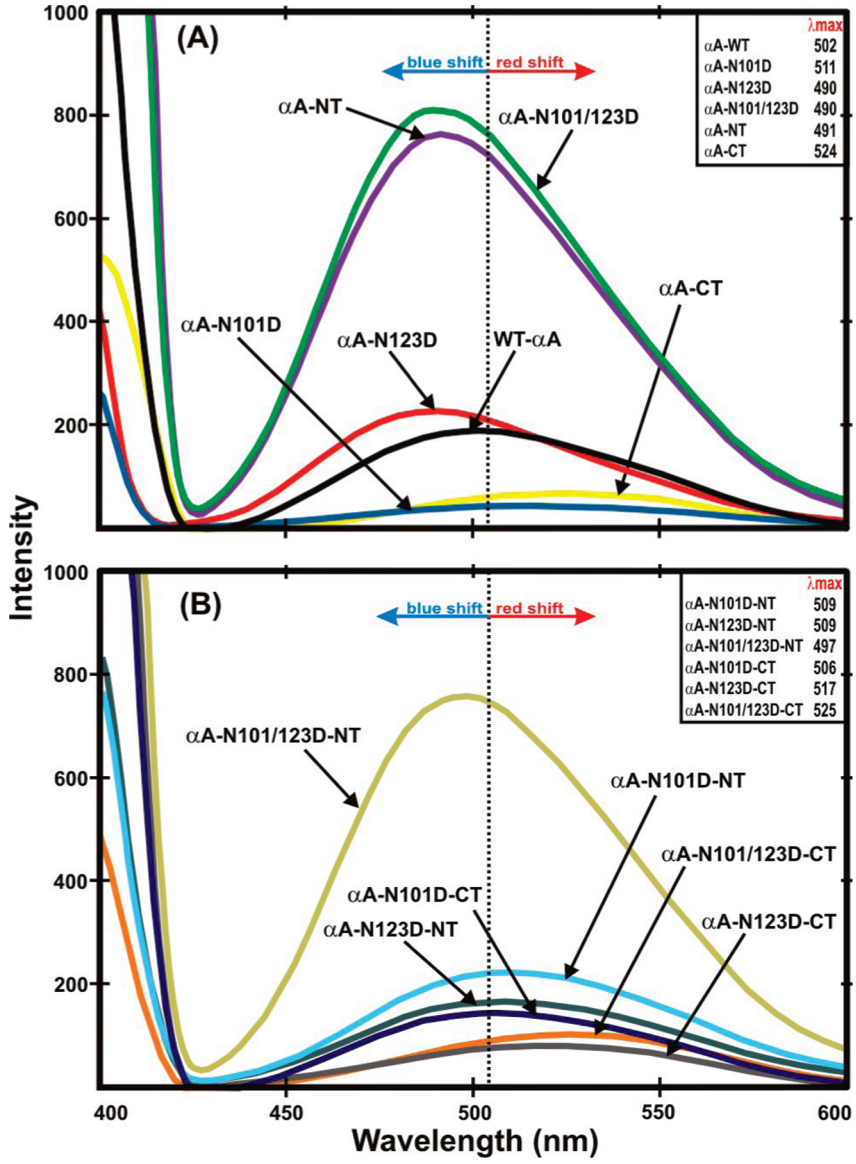

FIGURE 6: Fluoresence spectra (excitation at 390 nm and emission between 400 and 600 nm) of WT-αA and its mutant proteins after ANS binding. (A) WT-αA and its deamidated or truncated mutants. (B) The deamidated plus N- or C-terminally truncated mutants of WT-αA. The dotted line indicates the maximum wavelength peak observed in WT-αA to help establish whether a blue or red shift occurred after mutation.

red shift at λ_{max} of 509 nm in αA-N123D-NT and by a 15 nm red shift with quenching at 517 nm in αA-N123D-CT. Therefore, deamidation at N123 led to a relatively compact structure of the mutant, which was altered to a relaxed structure on deletion of either the N-terminal domain or C-terminal extension. Similarly, the λ_{max} of 490 nm of the αA-N101/123D mutant suggested a more compact structure relative to WT-αA. On N-terminal domain deletion, its λ_{max} was 497 with 7 nm red shift with quenching. On deletion of C-terminal extension, it exhibited λ_{max} of 525 nm with a red shift of 35 nm (Table 3). The data suggested that the deletion of either the N-terminal domain or C-terminal extension in the αA-N101/123D mutant resulted in a less compact structure than that of the αA-N101/123D mutant. Together, the results suggested that a deamidation-induced decrease in available hydrophobic surface patches was in the following order: αA-N101/123D > αA-NT > αA-N101/123D-NT > αA-N123D > αA-N101D-NT > WT-αA > αA-N123D-NT > αA-N101D-CT > αA-N101/123D-CT > αA-N123D-CT > αA-CT > αA-N101D.

(5) Subunit-Exchange Rates between WT-αB and WT-αA or Its Mutant Proteins. The subunit-exchange rates of heteromers containing WT-αB (labeled with Alexa fluor 488) and WT-αA (or its deamidated and/or N-terminal domain or C-terminal extension deleted mutants; labeled with Alexa fluor 350) were determined using the FRET method as described in Experimental Procedures. The subunit exchange rate (k) between WT-αB and WT-αA was 0.0412 min^{-1}, and it was used as 100% (control level) for the comparison of the exchange rates between WT-αB and αA mutant proteins (Table 3). Relative to the control, the subunit exchange rates of N-terminal domain-deleted or C-terminal extension-deleted αA and WT-αB were almost doubled (i.e., 170% and 180%, respectively). The subunit-exchange rates of αA-N101D, αA-N101D-NT, and αA-N101D-CT with WT-αB were 116%, 213%, and 197%, respectively, compared to the control. These results suggested increased subunit-exchange rates between αA with αB-crystallins on deamidation at N101, or on deamidation at N101 plus deletion of N-terminal domain or C-terminal extension.

However, reduced subunit exchange rates were seen between WT-αB and αA-N123D or αA-N123D-NT (i.e., 45%−54% compared to the control) but the same rate as in the control with the αA-N123D-CT mutant. The results suggested that either deamidation of N123 or deamidation plus N-terminal domain deletion had a major effect in reducing exchange rate with WT-αB, but no such effect was seen on the deletion of C-terminal extension in the deamidated αA. Interestingly, the subunit-exchange rate of αA-N101/123D significantly increased (183%), but the rates of subunit exchange of both αA-N101/123D-NT and αA-N101/123D-CT decreased to 63% and 84%, respectively, relative to the control.

(6) Determination of Molecular Mass by Static Light Scattering Method. The molecular masses of the homomers WT-αA, three deamidated αA species, and deamidated mutant proteins plus deletion of N-terminal domain or C-terminal extension were determined by static light scattering (Wyatt Technology). The molecular mass of proteins was determined using static/classical light scattering. The polydispersities and molecular masses of the proteins are reported in Table 3. The molecular mass of each species is shown in Table 3. Compared to the molecular mass of 7.0×10^5 Da of WT-αA protein, the three deamidated αA mutant proteins (αA-N101D, αA-N123D, and αA-N101/123D) showed molecular masses of 8×10^7, 6×10^5, and 1.5×10^8 Da, respectively. On deletion of the N-terminal domain, the molecular mass of the αA-NT decreased to 2.7×10^5 Da relative to WT. On similar deletion of the N-terminal domain in the three deamidated mutant proteins, the molecular masses of the αA-N101D-NT and αA-N123D-NT mutants were decreased to 3.4×10^5 and 7.9×10^4 Da, respectively, but increased to 3.8×10^7 Da for αA-N101/123D-NT mutant. The data suggested a crucial role of the N-terminal domain in oligomerization of αA subunits in homomers. In contrast, the deletion of the C-terminal extension caused an increase of mass on the αA-CT mutant to 1.15×10^8 Da relative to WT. A similar deletion of the C-terminal extension also increased mass in the three deamidated αA species (i.e., αA-N101D-CT, αA-N123D-CT, and αA-N101/123 Da showed mass of 4.0×10^7, 1.45×10^8, and 9.0×10^6 Da, respectively). Because the mass of the deamidated plus C-terminal extension deleted proteins were higher relative to identical species with deamidation alone, the deletion in αA facilitated subunit assembly in its homomers.

DISCUSSION

The major findings of the comparative studies of WT-αA and its mutant proteins are as follows: (1) The homomers of C-terminal extension (residues 140−173) deleted αA (αA-CT) became water insoluble (i.e., recovered in the inclusion bodies), whereas the N-terminal domain (residues 1−63) deleted αA species (αA-NT) remained water soluble. (2) In spite of structural instability and insolubilization of αA-crystallin upon deletion of the C-terminal extension, the protein showed almost no loss in functional (chaperone) property. However, the N-terminal domain-deleted αA-crystallin maintained the structural stability but showed significant loss in chaperone activity. (3) Among the αA-N101D, αA-N123D, and αA-N101/123D mutants, only the αA-N123D mutant showed maximum (complete) loss of chaperone activity on deamidation, suggesting that the N123 residue is critical for the chaperone activity of the crystallin. (4) Deletions of either the N-terminal domain or C-terminal extension in the deamidated αA-crystallin mutants led to recovery of chaperone activity, compared with activity in αA only with deamidation. The data suggested that alternative folding/subunit exchange of the deamidated crystallin on such deletions might be responsible for increase in chaperone activity. (5) Except for the αA-N101D-NT and αA-N101D-CT mutants, the chaperone activities of deamidated plus N-terminal domain- or C-terminal extension-deleted αA mutants (i.e., αA-N123D-NT, αA-N101/123D-NT, αA-N123D-CT, and αA-N101/123D-CT) were almost the same as the activity of WT-αA. Together, the data suggested that the deamidation alone showed a greater effect on chaperone activity than did the deletion of the N-terminal domain or C-terminal extension of αA-crystallin. (6) During heteromer formation, the αA-N123D and αA-N123D-NT mutants showed reduced subunit exchange rate with WT-αB, but such exchange rate was unaffected (i.e., remained at control levels [heteromers of WT-αA plus WT-αB]) on deletion of C-terminal extension. In contrast, similar heteromers of αA-N101D or αA-N101/123D with WT-αB exhibited gain in chaperone activity compared to the control. Together, the data suggested that subunit exchange rate might be among the factors affecting the chaperone activity levels.

The functional (chaperone activity) properties of N-terminal domain-deleted and C-terminal extension-deleted mutants (i.e., αA-NT and αA-CT) were consistent with their structural alterations as determined by various biophysical methods. The CD spectral results showed that αA-NT and αA-CT had increased β-sheet contents of 65% and 64%, respectively, compared to 45% of WT-αA. The α-helix content in αA-NT was almost the same as WT-αA (∼21−23%), but it was reduced to half (10%) in αA-CT protein. The results suggested that deletion of the N-terminal domain or C-terminal extension led to structural perturbation in αA-crystallin, but more so on the deletion of the latter. This could explain the structural instability of αA-CT leading to its insolubilization.

The intrinsic Trp fluorescence emission maximum in a protein is an index of Trp side chain exposure on the surface in a solvent, and generally the λ_{max} is at around 350 nm. Because αA contains only one Trp at position 9, which was lost on the deletion of N-terminal domain (residues 1−63) in the αA-NT mutant, the Trp fluorescence spectra of mutants lacking the N-terminal domain were not determined. Instead, the broad spectrum of these mutants was recorded. The αA-CT mutant that contained Trp-9 showed a red shift (λ_{max} of 348 compared to 345 in WT-αA), suggesting a relatively relaxed structure. On determination of broad spectra between 300 and 400 nm following excitation at 290 nm, the λ_{max} of WT-αA, αA-NT, and αA-CT were 345, 342, and 346 nm, respectively, suggesting a compact structure for αA-NT and relaxed structure for αA-CT relative to WT protein. These results were consistent with the CD spectral results and explain the unstable structure of the αA-CT mutant. These trends were also reflected from their ANS-binding results, which showed a four times greater intensity with 11 nm blue shift (decreased accessible surface hydrophobic patches) in αA-NT and three times lesser intensity with 22 nm red shift (greater accessible surface hydrophobic patches) in αA-CT

compared to the WT-αA-crystallin. The CD spectral results were further supported by their molecular mass results (i.e., increased molecular mass [1.2×10^8Da] of αA-CT compared to αA-NT [2.7×10^5 Da] and WT-αA [7.0×10^5 Da]). The observed decrease in molecular mass of αA-NT was consistent with a previous report showing that the N-terminal of α-crystallin is responsible for dimeric interaction, whereas the C-terminal regulates global quaternary structure and variability (*44*). Furthermore, that study (*44*) showed that although αA_{1-168} showed the same chaperone activity as the WT-αA, the subunit dynamics and the oligomerization were severely diminished. The increase in molecular mass of the αA-CT mutant on deletion of C-terminal 140−173 residues in our study was in contrast to a previous report (*45*), which showed a similar deletion resulted in reduction of molecular mass from 607 to 148 kDa. This could be attributed to the six His tags present in our recombinant αA-preparation. Additionally, the subunit exchange rates of αA-NT and αA-CT with WT-αB were two times greater than the rates between WT-αA and WT-αB crystallins. Therefore, the lesser exposure of hydrophobic patches and no loss of chaperone activity in αA-CT, but opposite results in αA-NT, were not consistent with their altered chaperone functions relative to WT-αA. This suggests that His tags might change protein properties, and data with His tag proteins needed careful interpretation.

Reports have suggested that, as in other sHSPs (*46*), the N-terminal domain of αA-crystallin is important for chaperone activity, self-assembly in oligomers, and structural stability. Our results also support these suggested properties of N-terminal domain of αA-crystallin. That is, deletion of the N-terminal domain resulted in altered structure with properties such as increased hydrophobic patches, β-sheet contents, and subunit exchange rate with WT-αB but reduced oligomer mass and chaperone activity. Residues 12−21 and 71−88 in the N-terminal domain of αA were identified as substrate binding sites (*47*). Similarly, two bis-ANS binding sites at residues 50−54 and 79−99 were also identified (*48*). Deletion of 1−63 amino acid residues in bovine αA-crystallin resulted in the formation of only a tetrameric species (*49*), suggesting severely diminished oligomerization property. This is consistent with the peptide scan results, which showed that residues 42−57 and 60−71 of αA play a role in oligomerization and subunit interactions (*10*). Further, both the N-terminal domain and C-terminal extension were shown to be important in the self-interaction of αA-crystallin (*50*).

Our results also showed that the deletion of the C-terminal extension in αA-crystallin resulted in its structural instability (as represented by its insolubilization, relaxed structure, decreased hydrophobic patches, and β-sheet contents, and increased oligomers mass) and increased chaperone activity. The increased chaperone activity with reduced structural stability of αA mutant needed to be studied further. The C-terminal extension of αA, because of the prevalence of mostly charged amino acids, acts as both solubilizer of target proteins (*46*) and as a structural stabilizer. On swapping of the C-terminal extensions of αA and αB crystallins, it was concluded that the unstructured C-terminal extension plays a crucial role in structural stability in addition to its solubilzer function (*51*). The C-terminal extension is also implicated in chaperone function because a decrease in chaperone activity of αA-crystallin was observed on either a specific deletion, introduction of hydrophobic amino acid residues, or immobilization of C-terminal extension (*52*). Apparently, the C-terminal extension of αA has a different function than that of αB, because the chimeric αB with C-terminal extension of αA showed enhanced chaperone activity, but the chimeric αA with C-terminal extension of αB almost lost the chaperone activity (*51*). It has also been shown that most mutations or truncations of the C-terminal extensions of α-crystallin and other α-sHSPs like HSP27 lead to pathology such as myofibrillar myopathy and cataract (*37, 46*).

One intriguing finding in this study was that the deamidation of N-123 resulted in complete loss of chaperone activity, and the deamidation severely affected the chaperone activity in the following order compared to the WT-αA: αA-N123D > αA-N101D > αA-N123/101D. The results were consistent with our previous report (*22*), which showed that both αA-N101D and αA-N123D mutants lost activity relative to WT-αA. However, a relatively greater loss in the activity of the αA-N123D mutant than the αA-N101D mutant in the present study could be due to presence of additional six His tags, which also affected the solubility of the αA-N123D and αA-N101D mutant proteins. Because WT-αA and all the other mutants that were studied in this report were His tagged, we attempted to normalize the effects of additional six His residues while comparing their structural and functional properties. Although some of the properties of αA-N101D and αA-N123D were different than WT-αA in the present study, the overall effects were similar to our previous report (*22*); i.e., structural and functional properties due to deamidation of N101 and 123 to D in αA were affected but at varying levels relative to WT-αA. Furthermore, several past studies that compared structural and functional properties of mutant crystallins to WT utilized His-tagged crystallins (*53, 54*).

As stated above, the deamidation alone showed a greater effect on chaperone activity than did the deletion of the N-terminal domain or C-terminal extension in the crystallin. This could be because N101 and N123 exist in the conserved αA-crystallin core region (residues 64−139), and their deamidation produced additional negative charges leading to altered protein conformation. This was consistent with the structural changes observed during the CD spectral analyses. Higher β-contents (β-sheet: 64−65%) on the deletion of N-terminal domain or C-terminal extension of αA-crystallin were seen, whereas the deamidation alone (without deletion) resulted in lower β-sheet contents (40%−43%) and relatively higher α-helix contents (30%−31% compared to 15%−16% of αA-NT and αA-CT). Whether the increased β-sheet contents in the αA species resulted in greater structural stability and whether increase in α-helix contents reduced the stability could not be assessed in these studies. Present literature suggests that the conserved α-crystallin core region (residues 64−139) of αA-crystallin also plays a role in its chaperone function and structural stability. A mutation in the conserved Arg residue (R116C) resulted in human congenital cataract (*13*) and in lens opacity and posterior suture defects in R116C transgenic mice (*55*), and reduced heteroaggregation with αB (*13*) and reduced chaperone activity (*56*), which suggests that the core region might also contribute to structural and functional properties of αA-crystallin.

The deamidated αA mutants (i.e., αA-N101D, αA-N123D, and αA-N101/123D) and N-terminal domain or C-terminal extension-deleted mutants (αA-NT and αA-CT) showed relatively greater loss in chaperone activity than the deamidated plus N-terminal domain-deleted or deamidated plus C-terminal extension-deleted αA mutants (i.e., αA-N101D-NT, αA-N123D-NT, αA-N101/123D-NT, αA-N101D-CT, αA-N123D-CT, and αA-N101/123D-CT). Furthermore, except for the αA-N101D-NT and αA-N101D-CT mutants, the chaperone activities of deamidated plus N-terminal domain or C-terminal extension-deleted αA mutants (i.e., αA-N123D-NT, αA-N101/123D-NT, αA-N123D-CT, and αA-N101/123D-CT) were almost at the same levels as the WT-αA. The loss or gain in functional property (chaperone activity) did not fully coincide with stability and structural changes in αA mutants compared to WT-αA-crystallin. The deamidated plus N-terminal domain-deleted αA mutants (i.e., αA-N101D-NT, αA-N123D-NT, and αA-N101/123D-NT) remained water soluble, whereas the C-terminal extension-deleted species (i.e., αA-N101D-CT, αA-N123D-CT, and αA-N101/123D-CT) became water insoluble (recovered in the inclusion bodies), which suggested that, in general, a greater structural instability on deletion of the C-terminal extension than on deletion of the N-terminal domain. Together, the results suggested although the deamidation showed a greater effect on chaperone activity than C-terminal deletion, the C-terminal extension plays a greater role in the structural stability of αA-crystallin than does the deamidation at N101 and/or N123 residues. The ANS binding data further supported the finding of increased chaperone activity and reduced structural stability results of αA mutants. The deamidated plus C-terminal extension-deleted αA species (αA-N101D-CT, αA-N123D-CT, and αA-N101/123D-CT) generally showed relative fluorescence quenching on ANS binding, with a red shift compared to both WT-αA and deamidated species (αA-N101D, αA-N123D, and αA-N101/123D). This suggested an increase in their exposed hydrophobic patches on deamidation and deletion.

The homoaggregates of αA- or αB-crystallins exchange subunits among themselves and with α-crystallin heteroaggregates (*56*), which leads to their dynamic structure and polydisperse character (*43*). Because the chaperone activity modulation is also dependent upon the subunit exchange rates, their packing in oligomers of varying sizes, and exposed surface hydrophobic patches (*4, 25, 52*), the subunit exchange rates between WT-αA, or its mutants with WT-αB, were determined. We maintained a 3:1 ratio (WT-αA or its mutants:WT-αB) in these studies for two reasons: (1) Although subunit exchange between αA- and αB-crystallin could occur at varying ratios, the 3 to 1 ratio of αA and αB was found to be the most thermostable and showed relatively more compact structure than the homomers of either WT-αA or WT-αB crystallins (*48, 57*). (2) A complex of WT-αA and WT-αB showed greater thermal stability than either protein alone; therefore, the complex is believed to have greater potential to protect proteins under stress (*48, 57*). The results in our study show that WT-αB, on oligomerization with αA-NT mutant, exhibited levels of chaperone activity almost identical to levels in the control (i.e., WT-αA:WT-αB, 3:1), but a similar oligomerization with αA-CT showed two times higher activity. As mentioned above, αA-NT had greater structural stability than αA-CT, but in the former, the deletion resulted in significant loss of chaperone activity. Therefore, increased chaperone activity in the heteromers of αA-NT and WT-αB might be due to αB being a better chaperone than αA (*73*), to αB being more flexible than αA-crystallin (*63*), and to the fact that increasing the content of αB relative to αA in heteromers increased chaperone activity (*59*).

Results presented herein also show that the chaperone activity that was lost in the two deamidated αA species (i.e., αA-N101D, αA-N123D) was recovered to the control levels (heteromers of deamidated αA and WT-αB). However, the heteromers of the αA-N101/123D mutant and WT-αB showed only 50% activity compared to the control level. Similarly, compared with heteromers of WT-αA and WT-αB crystallins, the heteromers containing deamidated αA showed higher molecular mass, altered tertiary structure, and reduced exposed hydrophobic surface and chaperone activity. Between the two Asn residues of αA-crystallin, only the Asn-123 and not the Asn-101 has been conserved in the mammalian species (*64*). Because deamidation introduces a negative charge, it is believed to cause alterations in protein tertiary structure, affecting their structural and functional properties. Although a frequent *in vivo* deamidation of Asn-101 and not of the Asn-123 residue has been reported in past studies (*36, 65*), our previous study (*23*) also showed relatively greater altered properties in the mutant αA-N101D than in the mutant αA-N123D compared to WT-αA-crystallin. Therefore, in the heteromers, the WT-αB-crystallin might provide greater surface hydrophobic patches to increase the chaperone activity of the deamidated mutant proteins. However, apparently, a similar effect did not occur in the heterooligomers of WT-αB and the αA-N101/123D mutant.

The chaperone activity of homomers composed of deamidated plus C-terminal extension-deleted αA mutants (αA-N101D-CT, αA-N123D-CT, and αA-N101/123D-CT) was at the same level as the WT-αA homomers. Further, the chaperone activity of the αA-CT plus WT-αB heteromer showed almost double the activity of the control, whereas the deamidated plus C-terminal extension-deleted species, on oligomerization with WT-αB-crystallin, lost about half of their chaperone activity. The results suggested that deletion of C-terminal extension was less deleterious than deamidation for maintaining the chaperone function even in heteromers of αA- and αB-crystallins.

In summary, the present study suggested that the deletion of the N-terminal domain or C-terminal extension in the deamidated αA-crystallin species resulted in major structural changes. The deamidation of N101 and N123 in αA showed greater effect on its chaperone activity than did deletion of either the N-terminal domain or C-terminal extension. The deletion of the C-terminal extension in WT-αA affected its structural stability, protein solubility, and oligomerization. The chaperone activity of N-terminal domain-deleted αA-homomers was reduced to the level of αA-N101D, but the maximum decrease occurred in the αA-N123D mutant compared to the WT-αA homomer. This suggested that both deletion of the N-terminal domain or mutation of N123 to D in αA-crystallin had a more pronounced effect on the chaperone activity than did deletion of the C-terminal extension of either WT-αA or deamidated αA mutants. However, these effects could not be fully explained by the

structural changes in the mutants. The present study emphasizes the importance of the above deletions vs deamidations on structural and functional properties of human αA-crystallin. Our future studies will be focused on whether these posttranslational modifications lead to cataract development in transgenic animals.

REFERENCES

1. Bloemendal, H., deJong, W., Jaenicke, R., Lubsen, N. C., Slingsby, C., and Tardieu, A. (2004) Ageing and vision: structure, stability and function of lens crystallins. *Prog. Biophys. Mol. Biol. 86*, 407–485.
2. Horwitz, J. (1992) α-Crystallin can function as a molecular chaperone. *Proc. Natl. Acad. Sci. U.S.A. 89*, 10449–10453.
3. Pasta, S. Y., Raman, B., Ramkrishna, T., and Rao, C. M. (2002) Role of C-terminal extension of α-crystallins; Swapping the C-terminal extension of αA-crystallin with αB-crystallin results in enhanced chaperone activity. *J. Biol. Chem. 277*, 45821–45828.
4. Takemoto, L., Emmons, T., and Horwitz, J. (1999) The C-terminal region of α-crystallin: involvement in protection against heat-induced denaturation. *Biochem. J. 294*, 435–438.
5. Bova, M. P., Mchaourab, H. S., Han, Y., and Fung, B. K. K. (2000) Subunit exchange of small heat shock proteins. Analysis of oligomer formation of αA-crystallin and HSP27 by fluorescence resonance energy transfer and site-directed truncations. *J. Biol. Chem. 275*, 1035–1042.
6. Aziz, A., Santhoshkumar, P., Sharma, K. K., and Abraham, E. C. (2007) Cleavage of C-terminal serine of human αA-crystallin produces αA_{1-172} with increased chaperone activity and oligomeric size. *Biochemistry 46*, 2510–2519.
7. Smulders, R. H. P. H., Carver, J. A., Lindner, E. A., van Bocket, M. A. M., Blomendal, H., and de Jong, W. W. J. (1996) Immobilization of the c-terminal extension of bovine αA-crystallin reduces chaperone-like activity. *J. Biol. Chem. 271*, 29060–29066.
8. Andley, U. P., Mathur, S., Griest, T. A., and Petrash, J. M. (1996) Cloning, expression, and chaperone-like activity of human αA-crystallin. *J. Biol. Chem. 271*, 31973–31980.
9. Sreelakshmi, Y., Santhoshkumar, P., Bhattacharyya, J., and Sharma, K. K. (2004) αA-crystallin interacting regions in the small heat shock protein, αB-crystallin. *Biochemistry 43*, 15785–15795.
10. Sreelakshmi, Y., and Sharma, K. K. (2006) The interaction between αA- and αB-crystalllin is sequence specific. *Mol. Vision 12*, 581–587.
11. Ghosh, J. G., and Clark, J. I. (2005) Insight into the domains required for dimerization and assembly of human αB-crystallin. *Protein Sci. 14*, 684–695.
12. Bova, M. P., Yaron, O., Huang, Q. L., Ding, L. L., Haley, D. A., Stewart, P. L., and Horwitz, J. (1999) Mutation R120G in αB-crystallin, which is linked to a desmin-related myopathy, results in an irregular structure and defective chaperone-like function. *Proc. Natl. Acad. Sci. U.S.A. 96*, 6137–6142.
13. Cobb, B. A., and Petrash, M. (2000) Structural and functional changes in the αA-crystallin R116C mutant in hereditary cataract. *Biochemistry 39*, 15791–15798.
14. Spector, A. (1984) The search for a solution to senile cataracts, Procter lecture. *Invest. Ophthalmol. Visual Sci. 25*, 130–145.
15. Nagaraj, R. H., Sell, D. R., Prabhakaram, M., Ortwerth, B. J., and Monnier, V. M. (1991) High correlation between pentosidine protein crosslinks and pigmentation implicates ascorbate oxidation in human lens senescence and cataractogenesis. *Proc. Natl. Acad. Sci. U.S.A. 88*, 10257–10261.
16. McDermott, M., Chiesa, R., Roberts, J. E., and Dillon, J. (1991) Photooxidation of specific residues in α-crystallin polypeptides. *Biochemistry 30*, 8653–8660.
17. Harrington, V., and Srivastava, O. P. (2007) Proteomics of crystallin species present in water insoluble proteins of normal and cataractous human lenses. *Mol. Vision 13*, 1680–1694.
18. Srivastava, O. P., and Srivastava, K. (2003) Existence of deamidated αB-crystallin fragments in normal and cataractous human lenses. *Mol. Vision 9*, 110–118.
19. Lorand L. (1988) Transglutaminase mediated cross-linking of proteins and cell aging: the erythrocyte and lens models, in *Advances in post-translational modifications of proteins and aging* (Zappia, V., Ed.) pp 79−94, Plenum Press, New York.
20. Wilmarth, P. A., Tanner, S., Dasari, S., Nagalla, S. R., Riviere, M. A., Bafna, V., Pevzner, P. A., and David, L. L. (2006) Age-related changes in human crystallins determined from comparative analysis of post-translational modifications in young and aged lens: Does deamidation contribute to crystallin insolubility? *J. Proteome Res. 5*, 2554–2566.
21. Lampi, K. J., Amyx, K. K., Ahmann, P., and Steel, E. A. (2006) Deamidation in human lens βB2 crystallin destabilizes the dimer. *Biochemistry 14*, 3146–3153.
22. Gupta, R., and Srivastava, O. P. (2004) Deamidation affects structural and functional properties of human αA-crystallin and its oligomerization with αB-crystallin. *J. Biol. Chem. 276*, 44258–44269.
23. Gupta, R., and Srivastava, O. P. (2004) Effect of deamidation of asparagine 146 on functional and structural properties of human lens αB-crystallin. *Invest. Ophthalmol. Visual Sci. 45*, 206–214.
24. Robinson, N. E. (2002) Protein deamidation. *Proc. Natl. Acad. Sci. U.S.A. 99*, 5283–5288.
25. Robinson, A. B., McKerrow, J. H., and Legaz, M. (1974) Sequence-dependent deamidation rates for model peptides of cytochrome c. *Int. J. Pept. Protein Res. 6*, 31–35.
26. Midelfort, C. F., and Mehler, A. H. (1972) Deamidation in vivo of an asparagine residue of rabbit muscle aldolase. *Proc Natl. Acad. Sci. U.S.A 69*, 1816–1819.
27. Lindner, H., Sarg, B., Hoertnagi, B., and Helliger, W. (1998) The microheterogeneity of mammalian $H1^0$ histone. Evidence for an age-dependent deamidation. *J. Biol. Chem. 273*, 1324–1330.
28. Inaba, M., Gupta, K. C., Kuwabara, M., Takahashi, T., Benz, E. J., Jr., and Maede, Y. (1992) Deamidation of human erythrocyte protein 4.1: Possible role in aging. *Blood 79*, 3355–3361.
29. van Kleef, F. S. M., Willems-Thijssen, W., and Hoenders, H. J. (1976) Intracellular degradation and deamidation of α-crystallin subunits. *Eur. J. Biochem. 66*, 477–483.
30. Groenen, P. J. T. A., van Dongen, M. J. P., Voorter, C. E. M., Bloemendal, H., and deJong, W. W. (1993) Age-dependent deamidation of αB-crystallin. *FEBS Lett. 322*, 69–72.
31. Takemoto, L., and Boyle, D. (2000) Specific glutamine and asparagines residues of gamma-S crystallin are resistant to in vivo deamidation. *J. Biol. Chem. 275*, 26109–26112.
32. Lund, A. L., Smith, J. B., and Smith, D. L. (1996) Modifications of the water-insoluble human lens α-crystallin. *Exp. Eye Res. 63*, 661–672.
33. Kim, Y. H., Kapfer, D. M., Boekhorst, J., Lubsen, N. H., Bachinger, H. P., Shearer, T. R., David, L. L., Feix, J. B., and Lampi, K. J. (2002) Deamidation, but not truncation decreases the urea stability of a lens structural protein, βB1-crystallin. *Biochemistry 41*, 14076–14084.
34. de Jong, W. W., van Kleef, F. S. M., and Bloemendal, H. (1974) Intracellular C-terminal degradation of αA chain of α-crystallin. *Eur. J. Biochem. 48*, 271–276.
35. Van Kleef, F. S. M., Willlems-Thyssen, W., and Hoenders, H. J. (1976) Intracellular degradation and deamidation of α-crystallin subunits. *Eur. J. Biochem. 66*, 477–483.
36. Srivastava, O. P., Srivastava, K., and Silney, C. (1994) Identification of origin of two polypeptides of 4 and 5 kDa isolated from human lenses. *Invest. Ophthalmol. Visual Sci. 35*, 207–214.
37. Selcen, D., Ohno, K., and Engel, A. G. (2004) Myofibrillar myopathy: clinical, morphological and genetic studies in 63 patients. *Brain 127*, 439–451.
38. Selcen, D., and Engel, A. G. (2003) Myofibrillar myopathies caused by novel dominant negative αB-crystallin mutation. *Ann. Neurol. 54*, 804–810.
39. Sun, Y., and MacRae, T. H. (2005) The small heat shock proteins and their role in human disease. *FEBS J. 272*, 2613–2627.
40. Laemmli, U. K. (1970) Cleavage of structural proteins during the assembly of bacteriophage T4. *Nature 227*, 680–685.
41. Sreerama, N., Venyaminov, S. Y., and Woody, R. W. (1999) Estimation of number of α-helical and beta strand segments in proteins using circular dichroism spectroscopy. *Protein Sci. 8*, 370–380.
42. Bera, S., Thampi, P., Cho, W. J., and Abraham, E. C. (2002) A positive charge preservation at position 116 of αA crystallin is critical for its structural and functional integrity. *Biochemistry 41*, 12421–12426.
43. Bova, M. P., Ding, L. L., Horwitz, J., and Fung, B. K. (1997) Subunit exchange of αA-crystallin. *J. Biol. Chem. 272*, 29511–29517.
44. Aquilina, J. A., Benesch, J. L. P., Ding, L. L., Yaron, O., Horwitz, J., and Robinson, C. V. (2005) Subunit exchange of polydisperse proteins. Mass spectrometry reveals consequences of αA-crystallin truncation. *J. Biol. Chem. 280*, 14485–144919.

45. Thampi, P., and Abraham, E. C. (2003) Influence of the C-terminal residues on oligomerization of αA-crystallin. *Biochemistry 42*, 11857–11863.
46. Evgrafov, O. V., Mersiyanova, I., Irobi, J., Van Den Bosch, L., Dierick, I., Leung, C. L., Schagina, O., Verpoorten, N., Van Impe, K., Fedotov, V., Dadali, E., Auer-Grumbach, M., Windpassinger, C., Wagner, K., Mitrovic, Z., Hilton-Jones, D., Talbot, K., Martin, J. J., Vasserman, N., Tverskaya, S., Polyakov, A., Liem, R. K., Gettemans, J., Robberecht, W., De Jonghe, P., and Timmerman, V. (2004) Mutant small heat-shock protein 27 causes axonal Charcot-Marie-Tooth disease and distal hereditary motor neuropathy. *Nat. Genet. 36*, 602–606.
47. Sharma, K. K., Kumar, R. S., Kumar, G. S., and Quinn, P. T. (2000) Synthesis and characterization of a peptide identified as a functional element in αA-crystallin. *J. Biol. Chem. 275*, 3767–3771.
48. Sharma, K. K., Kumar, G. S., Murphy, A. S., and Kester, K. (1998) Identification of 1,1′-Bi(4-anilino) naphthalene-5,5′-disulfonic acid binding sequence in α-crystallin. *J. Biol. Chem. 273*, 15474–15478.
49. Kantorow, M., Horwitz, J., van Boekel, M. A., deJong, W. W., and Piatigorsky, J. (1995) Conversion from oligomers to tetramers enhances autophosphorylation by lens αA-crystallin. *J. Biol. Chem. 270*, 17215–17220.
50. Fu, L., and Liang, J. J.-N. (2002) Detection of protein-protein interactions among lens crystallins in a mammalian two-hybrid system assay. *J. Biol. Chem. 277*, 4255–4260.
51. Kumar, L. V., and Rao, C. M. (2000) Domain swapping in human alpha A and alpha B crystallins affects oligomerization and enhances chaperone-like activity. *J. Biol. Chem. 275*, 22009–22013.
52. Datta, S. A., and Rao, C. M. (2000) Packing-induced conformational and functional changes in subunit of α-crystallin. *J. Biol. Chem. 275*, 41004–41010.
53. Cobb, B. A., and Petrash, J. M. (2000) Structural and functional changes in the αA-crystallin R116C mutant in hereditary cataracts. *Biochemistry 39*, 15791–15798.
54. Liu, B.-F., and Liand, J. J.-K. (2005) Interaction and biophysical properties of human lens Q155*-*β*B2 mutant. *Mol. Vision 11*, 321–327.
55. Hsu, C.-D., Kymes, S., and Petrash, J. M. (2006) A transgenic mouse model for human autosomal dominant cataract. *Invest. Ophthalmol. Visual Sci. 47*, 2036–2044.
56. Bera, S., and Abraham, E. C. (2002) The αA-crystallin R116C mutant has a higher affinity for forming heteroaggregates with αB-crystallin. *Biochemistry 41*, 297–305.
57. Bloemendal, M., and Bloemendal, H. (1998) Hydrophobicity and flexibility of αA- and αB-crystallin are different. *Int. J. Biol. Macromol. 22*, 239–245.

BI8001902